EXPERIMENTS WITH THE SASAMORI- AND THE ECMWF CLOUD COVER AND LIQUID WATER CONTENT PARAMETERIZATIONS

E. Heise

German Weather Service
Offenbach/Main FRG

1. INTRODUCTION

Most numerical models of the atmosphere calculate cloud cover from the relative humidity distribution, basically following Smagorinsky (1960). The optical properties of the clouds - required for the radiation calculation - are normally prescribed.

Leaving aside the possibility of a prognostic treatment of cloud liquid water content, only Sasamori (1975) has proposed a quite different scheme for the diagnostic determination of cloud cover and cloud liquid water content. His approach essentially takes into account the field of vertical velocity in addition to the relative humidity and temperature fields. A modification of this parameterization was tested by Hense (Hense, 1982; Hense and Heise, 1984 (Paper I)).

In this paper Sasamori's parameterization will be described and compared with the parameterization used in the operational model of the ECMWF (Geleyn, 1982). Results of global January simulation experiments will be presented.

2. SASAMORI'S STATISTICAL PARAMETERIZATION OF CLOUD COVER AND CLOUD LIQUID WATER CONTENT

Sasamori's basic assumption was that clouds in a slab of the atmosphere are generated by vertical motions of subgrid scale air parcels originating independently from different depths. A simple density distribution for the vertical displacements of the parcels forming the slab at one particular moment is assumed. A cloud model yields information about condensation processes and production of cloud liquid water in these parcels.

2.1 Cloud cover

Let us consider a layer of a numerical model of the atmosphere centered at $z = H_{N+1}$ (Figure 1). Cloud elements in this layer are formed by the air parcels which ascend from some depth x and reach their lifting condensation level at the height $z_s < H_{N+1}$ after travelling the distance $x_s(x) = z_s(x) - z(x)$. Parcels moving downward and parcels starting at depth x' with $z_s(x') \geq H_{N+1}$ do not contribute to the cloud cover in $z = H_{N+1}$. Integration over all parcels forming the layer under consideration yields for the cloud cover

$$\varepsilon_{N+1} = \int_0^{H_{N+1}} P(H_{N+1}, x)\, \theta(x - x_s(x))\, dx \qquad (1)$$

Here $P(H_{N+1}, x)dx$ is the relative number of air parcels in the layer with path length between x and x + dx, normalized by requiring

$$\int_{-\infty}^{H_{N+1}} P(H_{N+1}, x)\, dx = 1\,, \qquad (2)$$

and

$$\theta(\psi) = \begin{cases} 1 & , \psi > 0 \\ 0 & , \psi \leq 0 \end{cases}$$

The distance $x_s(x)$ (or the lifting condensation level $z_s(x)$) is computed from temperature T and relative humidity RH at depth x, assuming a dry adiabatic ascent. For the sake of simplicity, in each layer j of the numerical model only the values of T and RH in the center of the layer are used to compute one value x_{sj}, assumed to be constant throughout the layer. This allows (1) to be formulated as (compare Fig. 1)

$$\varepsilon_{N+1} = \sum_{j=1}^{N} \int_{a_j}^{h_{j+1}} P(H_{N+1}, x)\, dx \qquad (3)$$

where

$$a_j = \max\{h_j, \min\{x_{sj}, h_{j+1}\}\}$$

and (compare Paper I)

$$x_{sj} = -\frac{1}{f_j} \ln(RH_j) \qquad (4)$$

$$f_j = gL/(R_w c_p T_j^2) - g/(RT_j)$$

R_w is the gas constant for water vapour; the other symbols have their common meaning.

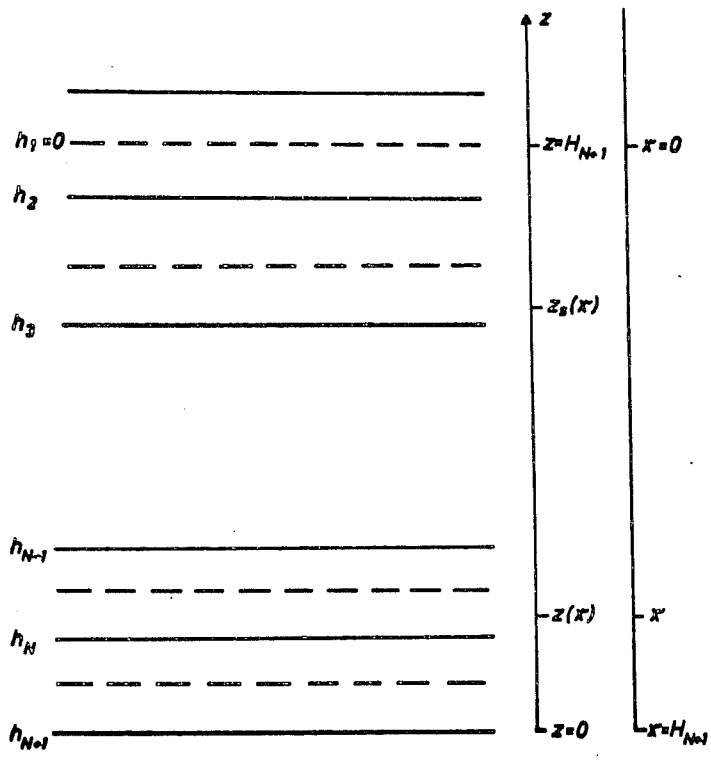

Figure 1: Coordinates used for the description of the Sasamori - parameterization.

Since there is no obvious physical reason for another distribution it is assumed that the origin of the parcels forming the layer at $z = H_{N+1}$ is given by a normal distribution with mean $\bar{x}$ and variance σ_x:

$$P(H_{N+1}, x) = \frac{1}{X_0(H_{N+1})} \exp\left[-\frac{1}{2}\left(\frac{x-\bar{x}}{\sigma_x}\right)^2\right] \tag{5}$$

and from (2)

$$X_0(H_{N+1}) = \int_{-\infty}^{H_{N+1}} \exp\left[-\frac{1}{2}\left(\frac{x-\bar{x}}{\sigma_x}\right)^2\right] dx \tag{6}$$

$\bar{x}$ and σ_x in (5) and (6) have to be replaced by variables computed during the GCM run. Sasamori (1975) argued that there is a high statistical correlation between the vertical path length of the air parcels and their vertical velocities. Taking an ensemble average over many air parcels, this correlation may be formulated as

$$x = \tau_w w \tag{7a}$$

$$\bar{x} = \tau_w \bar{w} \tag{7b}$$

$$\sigma_x = \tau_w \sigma_w \tag{7c}$$

where $\bar{w}$ is the mean vertical velocity and σ_w^2 the corresponding variance. τ_w is a time constant to be determined by tuning (see chapter 3).

In Paper I some possible methods for the determination of $\bar{w}$ and σ_w are summarized. Here the simplest one, the so-called 'mathematical parameterization', is used, i. e., mean value and variance of w in one grid element are estimated using the values of w in the grid element considered and in the 8 adjacent elements. Inserting (5) - (7) into (3) yields

$$\varepsilon_{N+1} = \left[\phi\left(\frac{H_{N+1}-\tau_w\bar{w}}{\tau_w\sigma_w}\right)\right]^{-1} \sum_{j=1}^{N}\left\{\phi\left(\frac{h_{j+1}-\tau_w\bar{w}}{\tau_w\sigma_w}\right) - \phi\left(\frac{a_j-\tau_w\bar{w}}{\tau_w\sigma_w}\right)\right\} \tag{8}$$

with

$$\phi(\psi) = (2\pi)^{-1/2} \int_{-\infty}^{\psi} e^{-t^2/2}\, dt \tag{9}$$

As the formulation of the normalization condition (2) leads to an unrealistic dependence of ε_{N+1} on σ_w if $\bar{x} \approx H_{N+1}$, only parcels originating from depths $H_{N+1} < x < (2\bar{x} - H_{N+1})$ are considered in the integration. The computed cloud cover distribution is not

altered significantly by this modification.

2.2 Cloud liquid water content

The air parcels are assumed to ascend moist adiabatically from the lifting condensation level to level H_{N+1}. During this ascent they build up cloud liquid water q_l and rain water. According to Sasamori (1975) the precipitation rate r is assumed to be proportional to the local mixing ratio of cloud liquid water:

$$r = q_e / \tau_p \tag{10}$$

where τ_p is a second time constant to be determined by numerical experimentation.

This parameterization of the precipitation rate leads to the following differential equation for q_l

$$\frac{dq_e}{dz} = \frac{c_p}{L}\left(\frac{g}{c_p} - \gamma_s\right) - \frac{1}{w}\frac{q_e}{\tau_p} \quad , \tag{11}$$

where γ_s is the moist adiabatic temperature gradient. Solving (11) for $z = H_{N+1}$ yields

$$q_e(H_{N+1}) = \frac{c_p}{L}\left(\frac{g}{c_p} - \gamma_s\right) w\tau_p \left\{1 - \exp\left(x - x_s(x)/(w\tau_p)\right)\right\} \tag{12}$$

Corresponding to (3) we define the ensemble mean of the cloud liquid water content at $z = H_{N+1}$ by

$$q_{e,N+1} = \sum_{j=1}^{N} \int_{a_j}^{h_{j+1}} q_e(H_{N+1})\, P(H_{N+1}, x)\, dx \tag{13}$$

The integration of (13) with (5),(7) and (12) is done with the aid of a piecewise linear approximation of the function $1 - \exp(x - x_s(x)/(w\tau_p))$ for short ($x_{s_j} \ll x$) and long ($x_{s_j} \approx x$) distances, resulting in

$$q_{e,N+1} = \frac{c_p/L}{\phi(H'_{N+1})} \sum_{j=1}^{N} \left(\frac{g}{c_p} - \gamma_{s_j}\right) \cdot \Bigg\{ \tag{14}$$

$$\frac{\tau_w \sigma_w}{\sqrt{2\pi}}\left(e^{-A_j^2/2} - e^{-B_j^2/2}\right) + \left(\tau_w \bar{w} - x_{s_j}\right)\left[\phi(B_j) - \phi(A_j)\right] +$$

$$\frac{\tau_p \sigma_w}{\sqrt{2\pi}}\left(1 - e^{-\frac{\tau_w}{\tau_p}}\right)\left(e^{-B_j^2/2} - e^{-H_{j+1}^2/2}\right) + \left[\tau_p \bar{w}\left(1 - e^{-\frac{\tau_w}{\tau_p}}\right) - x_{s_j} e^{-\frac{\tau_w}{\tau_p}}\right]\left[\phi(H_{j+1}) - \phi(B_j)\right] \Bigg\}$$

with

$$H'_{N+1} = \left(H_{N+1} - \tau_w \bar{w}\right)/\tau_w \sigma_w$$

$$A_j = (a_j - \tau_w \bar{w}) / \tau_w \sigma_w$$

$$B_j = (b_j - \tau_w \bar{w}) / \tau_w \sigma_w$$

$$H_{j+1} = (h_{j+1} - \tau_w \bar{w}) / \tau_w \sigma_w$$

and

$$b_j = x_{sj} (1 - e^{-\tau_w/\tau_p}) / [1 + \frac{\tau_p}{\tau_w} (e^{-\tau_w/\tau_p} - 1)]$$

In equation (14) the terms proportional to σ_w represent the influence of the subgrid-scale vertical velocities, while the other terms come from the mean vertical motions. The terms in the second line originate from parcels ascending over short distances, those of the third line from parcels ascending over long distances.

3. TUNING

Figure 2 and Table 1 show results of the tuning of the Sasamori-scheme. Additionally, comparable values for the ECMWF-scheme are displayed. This latter scheme computes cloud cover and cloud liquid water content from

$$\varepsilon = \begin{cases} \left[\frac{RH - RH_c}{1 - RH_c}\right]^2 & , RH > RH_c \\ 0 & \text{else} \end{cases} \qquad (15)$$

where

$$RH_c = 1 - \alpha\sigma(1-\sigma)(1+\beta(\sigma - 0.5))$$

$$\sigma = p/p_* \; , \; \beta = \sqrt{3}$$

and

$$q_e = \gamma \cdot q_{sat}(T, p) \qquad (16)$$

with the two tuning parameters α and γ (β has not been changed).

The global data set required for the tuning was taken from day 48 of GCM-Experiment 15I (see below). The tuning of α and γ for this experiment had been done partly with other observations and - of course - with another data set.

Using one single data set, for both schemes the global mean value of cloud cover ε may be determined by only one tuning parameter (τ_w and α, respectively). By and large ε is proportional to the tuning parameter. On the other hand, the dependence

Sasamori									ECMWF								
				p=0			surface						p=0			surface	
τ_w [sec]	τ_p [sec]	ε [%]	q_ℓ [g/m²]	LW↑ [W/m²]	SW↑ [W/m²]	Albedo [%]	LW↓ [W/m²]	SW↓ [W/m²]	α	γ	ε [%]	q_ℓ [g/m²]	LW↑ [W/m²]	SW↑ [W/m²]	Albedo [%]	LW↓ [W/m²]	SW↓ [W/m²]
5000	250	39.6	3.4	233.9	85.8	25.0	301.6	221.0	0.50	0.003	31.5	10.3	233.2	88.2	25.7	306.7	215.5
7500	250	41.9	5.0	233.1	88.8	25.9	302.5	216.0	0.75	0.003	38.9	13.9	230.9	96.7	28.2	310.5	200.2
10000	250	43.8	8.1	232.3	91.6	26.7	303.3	211.2	1.00	0.003	45.8	18.1	228.6	104.5	30.5	314.5	185.5
12500	250	45.6	12.6	231.5	94.4	27.6	304.2	206.4	1.25	0.003	52.2	22.5	226.4	112.1	32.7	318.4	171.3
15000	250	47.1	18.5	230.6	97.1	28.3	305.2	202.0	1.50	0.003	58.0	27.0	224.3	119.2	34.8	322.3	158.0
17500	250	48.6	25.5	229.7	99.7	29.1	306.2	197.7	1.75	0.003	63.3	31.4	222.4	125.4	36.6	326.1	146.2
20000	250	49.8	33.4	228.8	102.2	29.8	307.2	193.6	2.00	0.003	68.1	35.7	220.5	130.9	38.2	329.8	136.4
5000	500	39.6	6.6	230.4	91.1	26.6	304.4	213.9	0.50	0.006	31.5	20.6	230.6	93.1	27.2	309.6	208.8
7500	500	41.9	8.6	229.4	94.2	27.5	305.4	208.8	0.75	0.006	38.9	27.9	227.8	102.8	30.0	312.7	191.9
10000	500	43.8	12.0	228.5	96.9	28.3	306.4	204.1	1.00	0.006	45.8	36.2	225.2	111.5	32.5	316.9	175.6
12500	500	45.6	16.8	227.7	99.6	29.1	307.3	199.5	1.25	0.006	52.2	45.0	222.6	119.8	35.0	321.1	160.0
15000	500	47.1	23.0	226.8	102.2	29.8	308.3	195.3	1.50	0.006	58.0	53.9	220.1	127.5	37.2	325.2	145.7
17500	500	48.6	30.2	226.0	104.6	30.5	309.2	191.2	1.75	0.006	63.3	62.8	217.8	134.3	39.2	329.1	133.4
20000	500	49.8	38.3	225.1	107.0	31.2	310.1	187.3	2.00	0.006	68.1	71.3	215.6	140.2	40.9	333.0	122.6
5000	1000	39.6	12.6	226.6	96.6	28.2	307.2	206.5	0.50	0.012	31.5	41.2	228.4	98.2	28.7	310.0	202.4
7500	1000	41.9	15.6	225.4	100.0	29.2	308.4	201.0	0.75	0.012	38.9	55.8	225.2	108.8	31.8	314.2	184.0
10000	1000	43.8	19.6	224.4	102.8	30.0	309.5	196.1	1.00	0.012	45.8	72.4	222.3	118.4	34.6	318.5	166.6
12500	1000	45.6	25.1	223.4	105.4	30.8	310.5	191.6	1.25	0.012	52.2	90.1	219.4	127.3	37.2	322.8	150.0
15000	1000	47.1	31.8	222.5	107.8	31.5	311.5	187.6	1.50	0.012	58.0	107.9	216.7	135.6	39.6	327.0	134.9
17500	1000	48.6	39.5	221.7	110.1	32.1	312.4	183.7	1.75	0.012	63.3	125.5	214.2	142.8	41.7	331.0	122.2
20000	1000	49.9	48.1	220.8	112.4	32.8	313.3	179.9	2.00	0.012	68.1	142.7	211.7	149.2	43.5	334.9	110.9
Hoyt Model C:		44.1	134	236.6	105.8	30.1	316.2	188.6			44.1	147	236.6	105.8	30.1	316.2	188.6

	Experiment	Hoyt, Model C
Insolation at top of the atmosphere [W/m²]	342.6	351.3
Upward LW radiation at the surface [W/m²]	380.3	391.4
Albedo of the surface [%]	13.5	12.6

Table 1: Tuning of the Sasamori-scheme and comparable results for the ECMWF-scheme. Global mean values of cloud cover (ε), liquid water content of clouds (q_l), upward longwave (LW↑) and shortwave (SW↑) radiation at the top of the atmosphere, planetary albedo, downward longwave (LW↓) and shortwave (SW↓) radiation at the surface of the earth. Results of Hoyt (1976) for comparison.

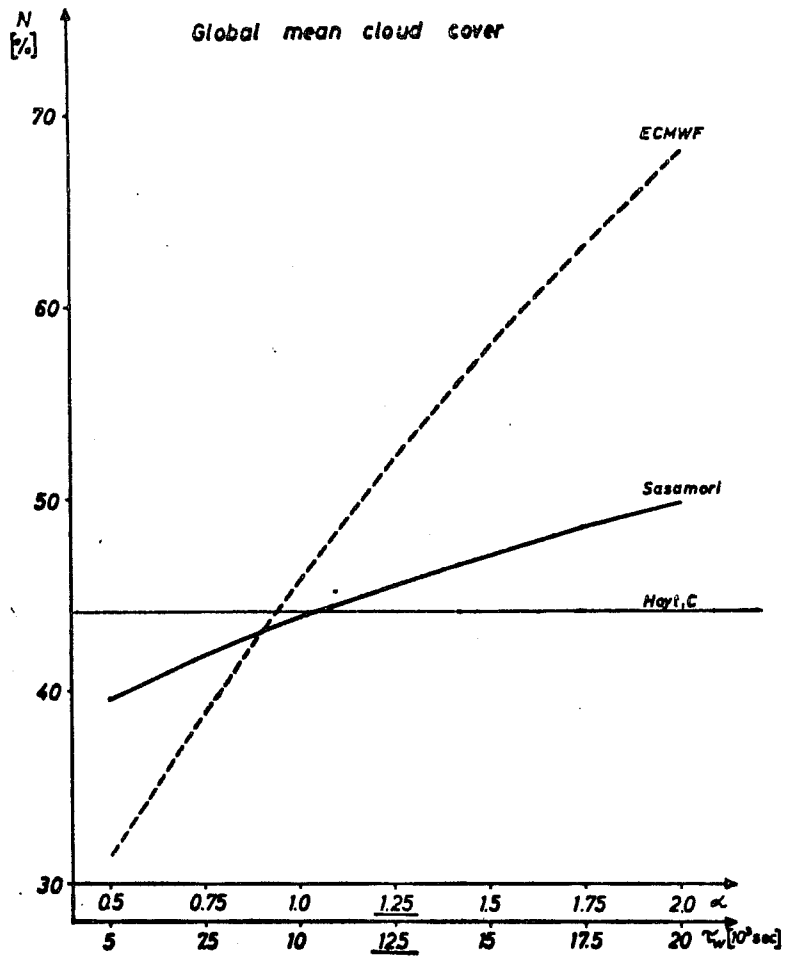

Figure 2a

Figure 2: Tuning of the Sasamori-scheme and comparable results for the ECMWF-scheme. Results of Hoyt (1976) for comparison.

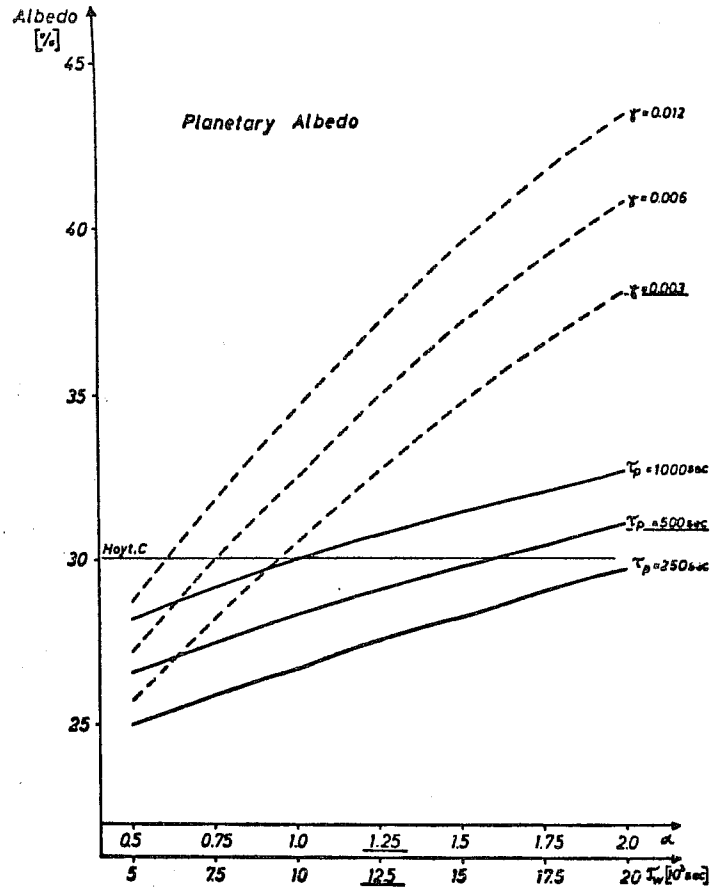

Figure 2b

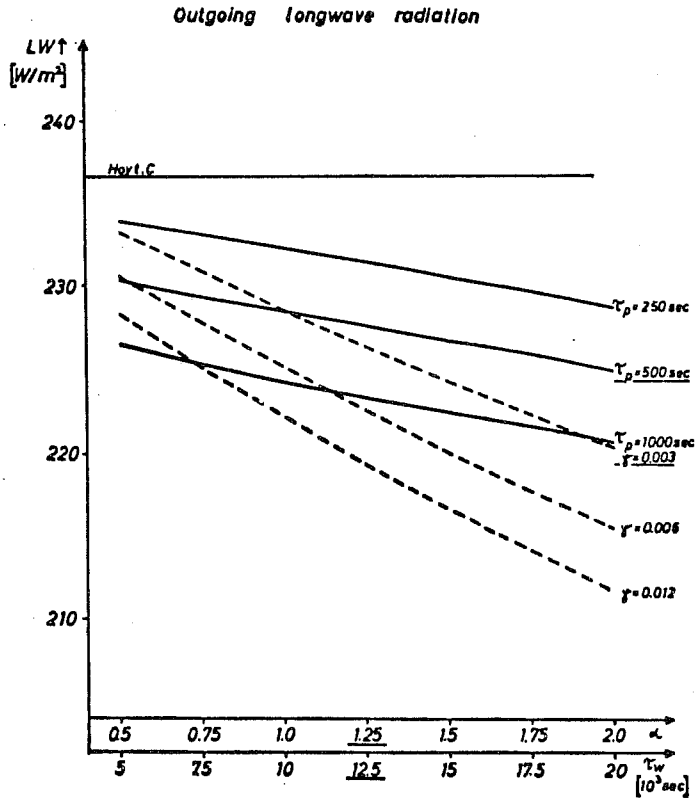

Figure 2c

of cloud liquid water content on the tuning parameters is quite different in the two parameterizations. Whereas in the ECMWF-scheme q_l is proportional to γ for all values of α, a corresponding relation for the Sasamori-scheme holds only for small values of τ_w. With increasing values of τ_w the dependence of q_l on τ_p decreases.

Of course, it is not possible to adjust all radiation balance components and cloud cover and liquid water content towards their climatological values (as far as these are known) by tuning two free parameters. Most emphasis was given to a correct simulation of cloud cover, planetary albedo and outgoing longwave radiation. The combination τ_w = 12500 sec and τ_p=500sec is a compromise in approaching Hoyt's (1976) model C values. Up to now a systematic test of the influence of different vertical profiles of τ_w and/or τ_p has not been performed. Using properly chosen vertical profiles a better representation of other radiation balance components might be possible.

As may be seen from Table 1 the combination chosen for τ_w and τ_p results in very small values of the global mean liquid water content of clouds. This remains true even if the measurements by Njoku and Swanson (1983) are used for the comparison. They estimate a value of roughly 70 g/m^2. Presumably the small value, which is required by the radiation code in order to give realistic values to the radiation balance components, uncovers a shortcoming of this code. This conjecture is supported by some results of Roeckner (in this Report), who uses the same radiation code.

4. EXPERIMENTS

January simulation experiments have been performed using the global C-grid general circulation model of the German Weather Service. The difference system of the model is essentially the same as the one given by Burridge and Haseler (1977). An early version of the model physics was described by Tiedtke and Geleyn (1975); major changes concern the radiation code (Hense et al., 1982) and the prediction of land surface temperatures (Jacobsen and Heise, 1982). The resolution chosen for the experiments is 10 layers in the vertical, equally

spaced in $\sigma = p/p_*$, and $\Delta\lambda = \Delta\varphi = 5^o$. The integrations start from analyses of Dec. 16th, 1978, and are continued up to the end of January.

Results of two experiments will be presented: i) Exp. 15I, using the ECMWF-scheme, with $\alpha = 1.25$ and $\gamma = 0.003$, and ii) Exp. 22, using the Sasamori-scheme with $\tau_w = 12500$ sec and $\tau_p = 500$ sec. No attempt was made to take into account convective cloud cover in either of these experiments.

In addition to the standard model diagnostics, single time step forecasts were made at several model days to allow for some further diagnostics. For both experiments the ECMWF-scheme and the Sasamori-scheme were used. Here the parameters $\alpha = 1.0$ and $\gamma = 0.002$ were taken for the ECMWF-scheme. This facilitates the comparison of the results (compare Fig. 2 and Table 1).

5. RESULTS

Table 2 contains global mean values of cloud cover, liquid water content and radiation balance components obtained by the single time step analyses. Remarkable are the liquid water content values at day 32 (Exp. 22) and 40 (Exp. 15I) diagnosed by the Sasamori-scheme. They are quite different from the values at the other days, although cloud cover and ECMWF-results are fairly constant. Some details of the results at days 28 and 32 (Exp. 22) are shown in Fig. 3. Whereas the zonal mean distribution of cloud cover is very similar at both days, there are large differences in the distribution of cloud liquid water content, especially between 15^oN and 50^oN. As the respective distributions obtained using the ECMWF-scheme (not displayed) don't indicate similar differences, we can assume that the field of relative humidity remained nearly unchanged. A possible reason for the reduction of cloud liquid water at day 32 is the much smaller value of the standard deviation of vertical velocity (Figure 3b). Large values of the standard deviation prevent large values of cloud cover but allow parcels to reach the layer considered by ascending from great depths. Thereby they produce high values of liquid water. A corresponding reasoning holds for day 40 of Exp. 15I.

In Fig. 4 the geographical distribution of cloud cover is

		Sasamori					ECMWF				
day		ε [%]	q_ℓ [g/m^2]	LW↑ [W/m^2]	SWnet [W/m^2]	Albedo [%]	ε [%]	q_ℓ [g/m^2]	LW↑ [W/m^2]	SWnet [W/m^2]	Albedo [%]
16	Exp.22	45.5	13	224	246	28.1	49.9	17	226	240	30.0
20		47.3	14	223	249	27.4	49.7	18	225	238	30.5
24		47.3	16	223	246	28.2	52.8	19	224	232	32.4
28		49.9	16	223	242	29.5	53.7	20	224	227	33.6
32		50.0	10	223	244	28.8	54.2	20	224	232	32.4
36		48.3	14	223	248	27.7	54.2	20	224	233	32.0
40		47.0	13	224	248	27.7	50.7	19	225	236	31.1
44		49.2	14	224	247	28.0	51.7	19	225	237	30.8
48		47.6	14	223	251	26.6	50.6	19	225	242	29.3
mean		48.3	14	223	247	28.0	51.9	19	225	235	31.3
32	Exp.15I	46.5	18	227	244	28.7	46.4	11	229	241	29.7
36		45.6	18	227	242	29.4	45.1	11	230	242	29.4
40		43.5	26	228	244	28.9	41.0	11	233	246	28.1
44		44.5	19	228	243	29.0	44.1	12	231	240	29.8
48		45.5	17	228	243	29.0	45.8	12	231	242	29.3
mean		45.1	20	228	243	29.0	44.5	11	231	242	29.3

Table 2: Single time step analyses of experiments 15I and 22 with both the Sasamori- and the ECMWF-schemes. Notations as in Table 1, SW_{net} = net radiation at the top of the atmosphere.

compared with observations (Berlyand and Strokina, 1980). The coarse structure is rather similar in both experiments, but major differences occur over South America, South Africa and Australia, where in Exp. 22 the cloud cover is considerably lower than in Exp. 15I. Compared to the observations over South America and South Africa, the ECMWF-simulation seems to be superior. The high cloud cover values off the eastern coast of Africa - simulated with both parameterizations - don't show up in the observations. High values are expected in the northern parts of the Atlantic and Pacific oceans; in these regions the Sasamori-scheme agrees somewhat better with the observations. Rather low cloud cover over the north polar basin is not simulated in either of the experiments, whereas the minimum over Antarctica appears, although its extension is too large.

Both parameterizations yield excessive meridional variations of cloud cover (Figure 5), but they fail in reproducing the observed polar minima. Over the southern hemisphere the midlatitude values are too small. This might be a consequence of the too weak eddy activity in the simulations. The much too high tropical values in Exp. 22 seem to be a problem of this particular experiment. The single time step analysis using the ECMWF-scheme yields even larger cloud cover values (81 %), and the respective analysis of Exp. 15I using the Sasamori-scheme gives 60 % cloud cover.

Taking into account convective cloud cover too, would certainly alter the distribution of zonal mean cloudiness. This seems to be a necessary step before altering the parameterization of largescale clouds.

The geographical distribution of the liquid water content of clouds can be shown for Exp. 22 only (Figure 6). Compared to observations (Njoku and Swanson, 1983) the high values over the tropical oceans are quite realistic but should be more concentrated along zonal bands. The maxima over the midlatitude oceans are far too weak in the experiments. This becomes evident in the zonal mean values (Figure 7), where only in the northern midlatitudes is there a small maximum in Exp. 22.

The zonal mean liquid water content distribution for the Sasa-

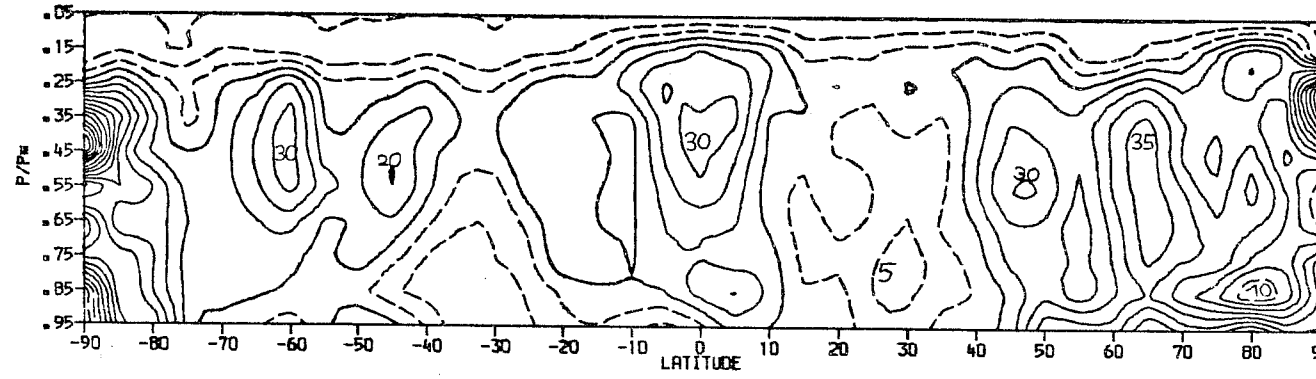

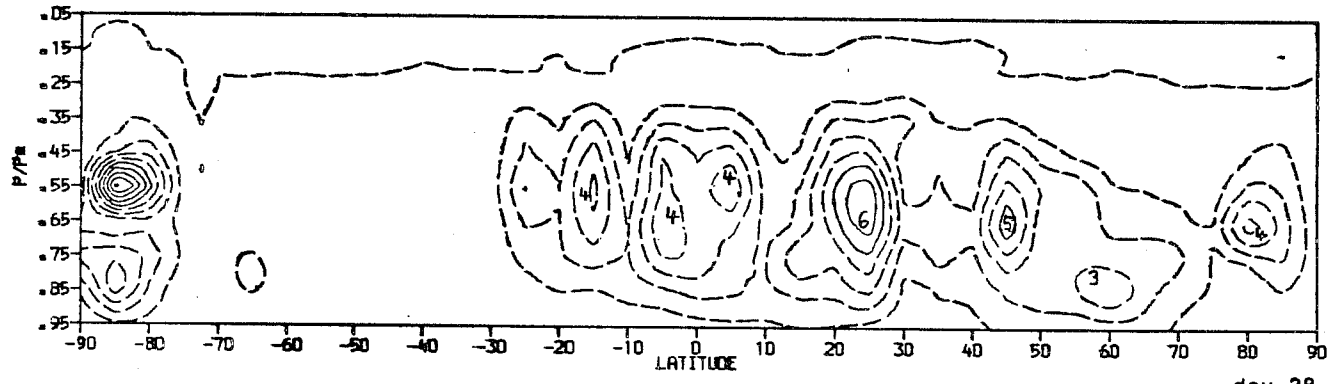

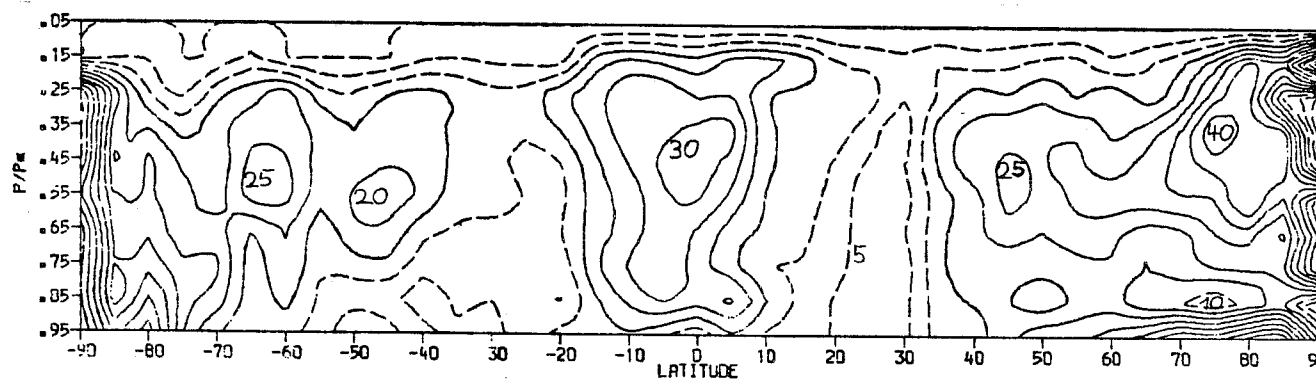

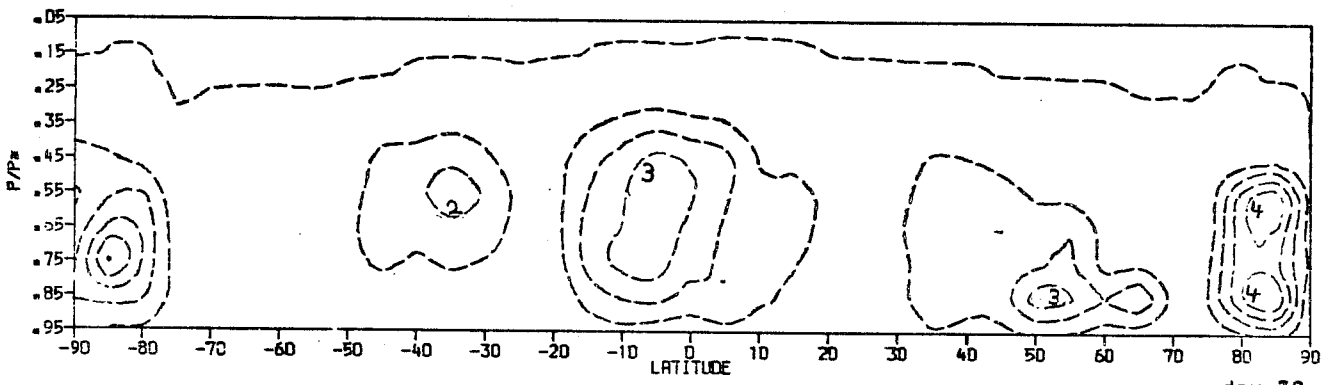

Figure 3: a) Zonal mean values of cloud cover and cloud liquid water content obtained by single time step analyses of day 28 and day 32 of Exp. 22 using the Sasamori-scheme. Units: Cloud cover in %, liquid water content in 10^{-3} g/m^3.
b) Vertical velocity and standard deviation of vertical velocity at day 28 and day 32 of Exp. 22. (mm/sec).

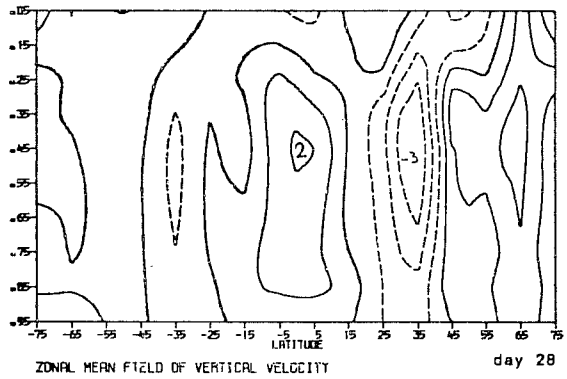
2
-3
LATITUDE
ZONAL MEAN FIELD OF VERTICAL VELOCITY
day 28

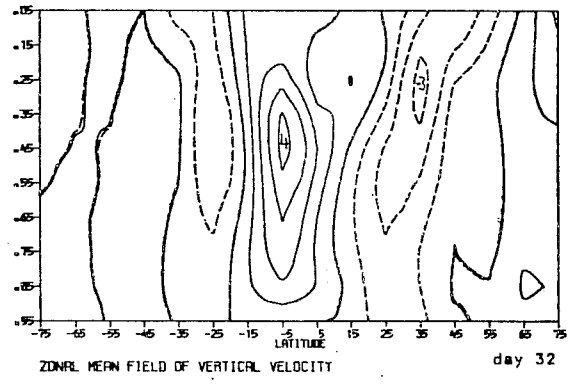
4
LATITUDE
ZONAL MEAN FIELD OF VERTICAL VELOCITY
day 32

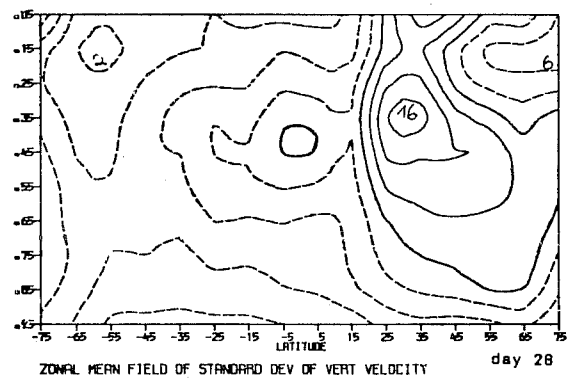
2
6
16
LATITUDE
ZONAL MEAN FIELD OF STANDARD DEV OF VERT VELOCITY
day 28

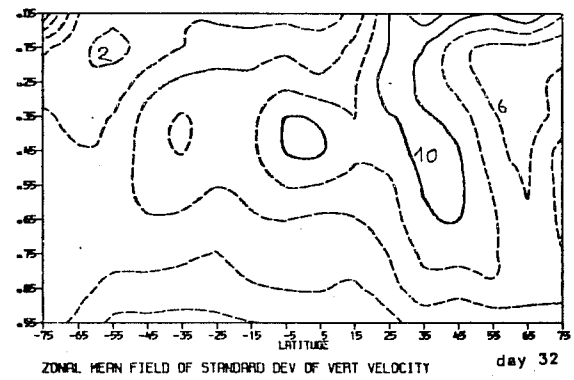
2
6
10
LATITUDE
ZONAL MEAN FIELD OF STANDARD DEV OF VERT VELOCITY
day 32

Figure 3b

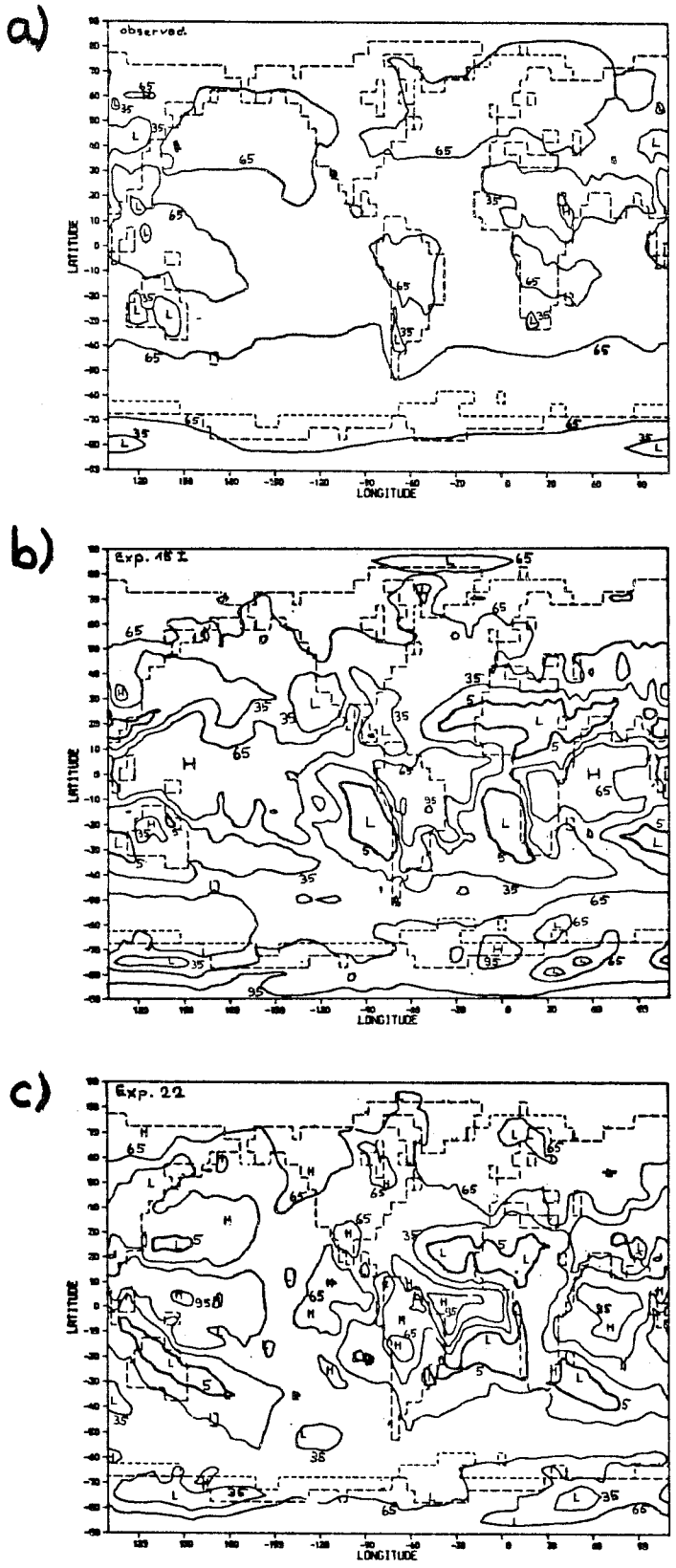

Figure 4: January distribution of cloud cover (%). a) observed (Berlyand and Strokina, 1980), b) Exp. 15I, c) Exp. 22

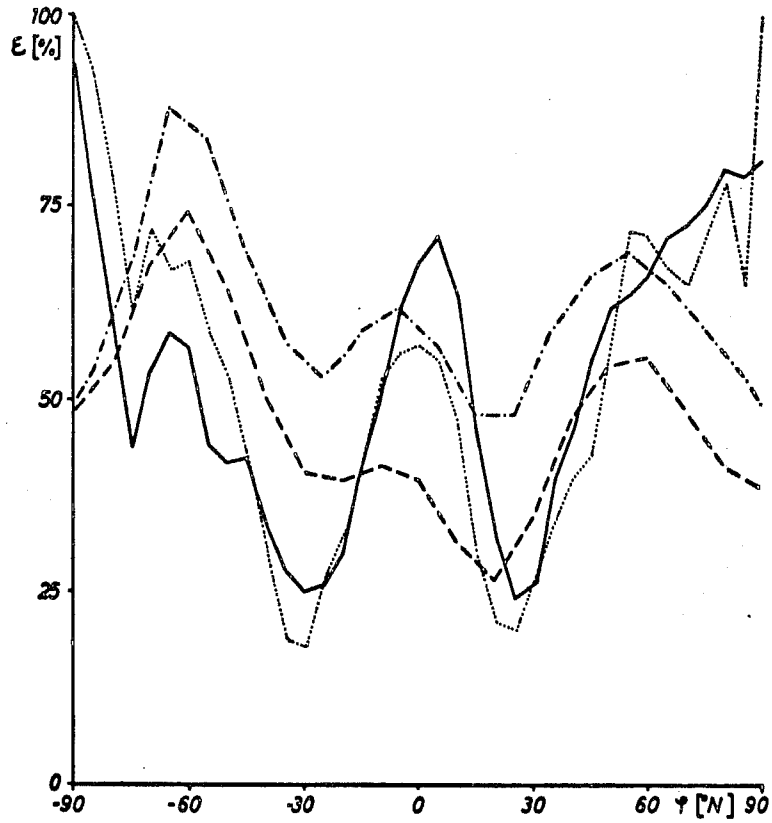

Figure 5: January zonal mean cloud cover, -·-·- observed (Berlyand and Strokina, 1980), – – – observed (Hoyt, 1976), ····· Exp. 15I (single time step analyses of days 32,36,40, 44 and 48), ——— Exp. 22.

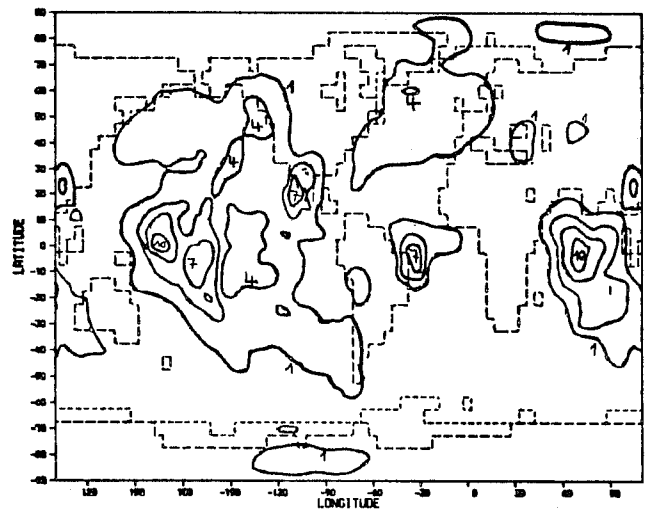

Figure 6: January distribution of cloud liquid water content Exp. 22 (10^{-3} g/cm^2).

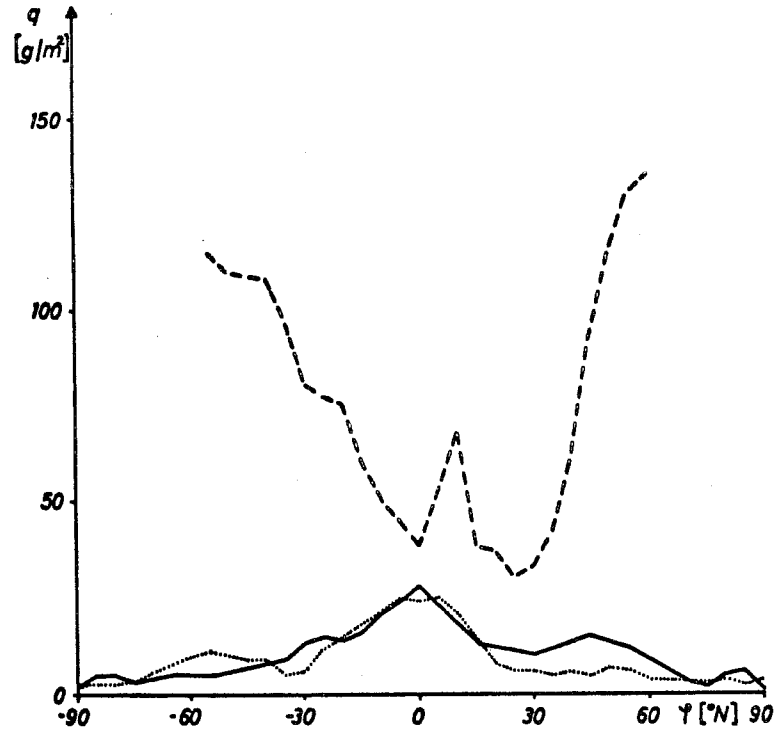

Figure 7: Zonal mean liquid water content, – – – observed (Njoku and Swanson, 1983), ····· Exp. 15I (single time step analyses as in Fig. 5), ——— Exp. 22

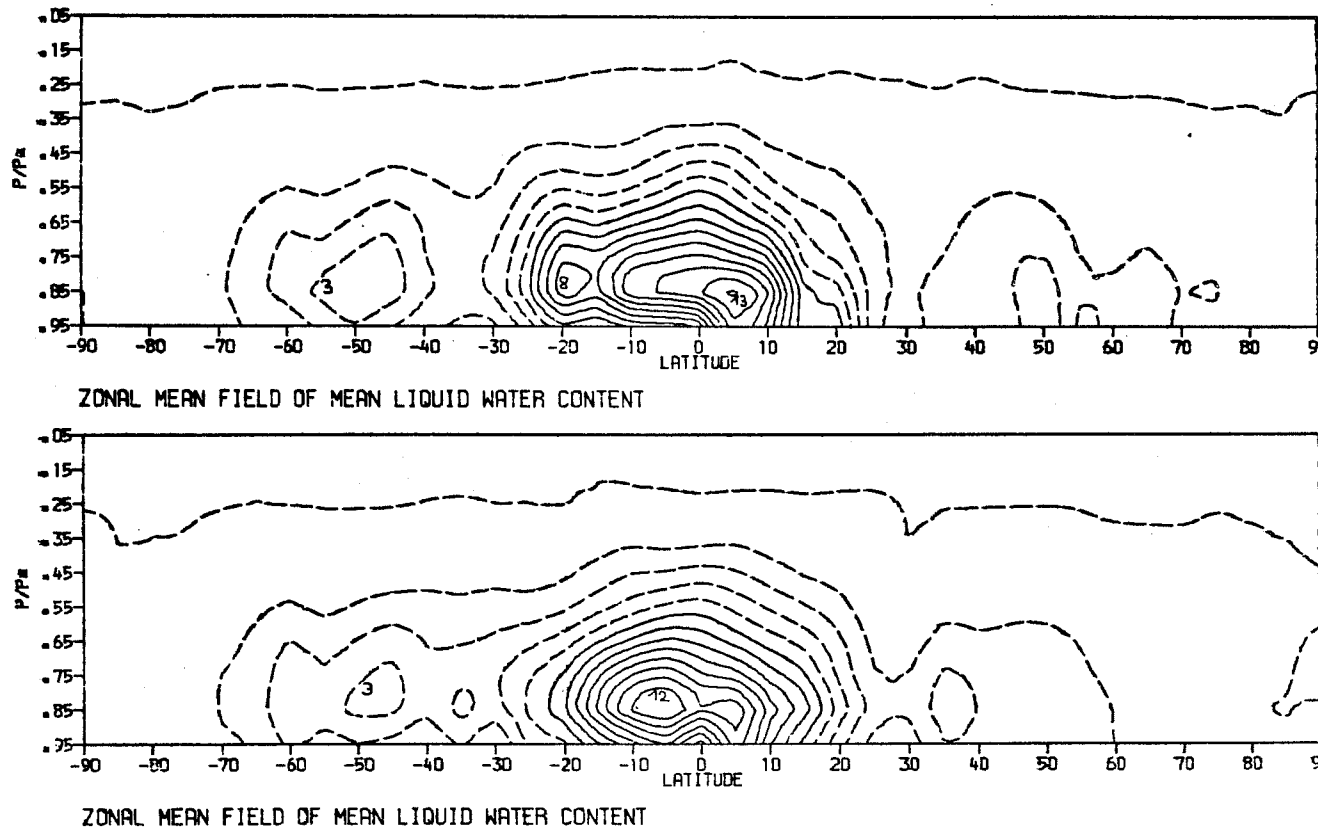

Figure 8: Zonal mean distribution of cloud liquid water content (10^{-3} g/m^3) obtained by single time step analyses of day 28 (upper part) and day 32 (lower part) of Exp. 22 using the ECMWF-scheme.

mori-scheme presented in Fig. 3a may be compared with corresponding distributions for the ECMWF-scheme (Figure 8). As the zonal mean cloud cover obtained by the single time step analysis of Exp. 22 using the ECMWF-scheme is 10 to 15 % higher than using the Sasamori-scheme (except between 20^{o}N and 60^{o}N, where it is 2 to 5 % lower), the absolute values of zonal mean cloud liquid water content are not comparable. Typically the Sasamori-scheme predicts maxima at greater heights, and presumably greater values in northern midlatitudes.

Up to now these distributions cannot be verified by observations. The results of Njoku and Swanson (1983) suggest that in tropical latitudes both schemes perform rather well. In northern midlatitudes the Sasamori-scheme seems to be slightly superior. In southern midlatitudes the Sasamori-scheme is hampered even more than the ECMWF-scheme by the model deficiency of too weak eddy activity.

The zonal mean distributions obtained by the Sasamori-scheme show a greater variability in time compared to those obtained by the ECMWF-scheme, because q_1 depends not only on the relatively slowly varying fields of temperature and pressure but additionally on the more variable fields of vertical motion.

Figure 9 demonstrates the influence of cloud cover and liquid water content on the shortwave radiation balance at the top of the atmosphere. The zonal mean albedo values directly reflect the effect of too large cloud cover in tropical latitudes, and too small cloud cover and liquid water content values in midlatitudes.

In tropical latitudes the errors in the shortwave radiation balance are partly compensated by the errors in the longwave radiation balance, therefore the observed net radiation balance is reproduced quite well (Figures 10 and 11). In northern midlatitudes too, the net radiation balance is simulated reasonably well. On the other hand, there are large errors in the southern midlatitudes, where the errors in short- and longwave radiation act in the same direction.

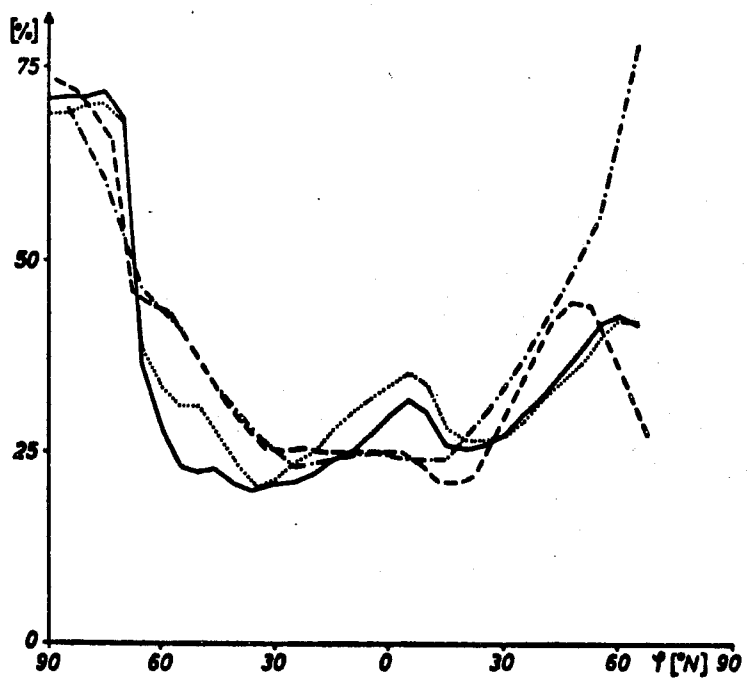

Figure 9: January mean planetary albedo, —·—· observed (Stephens et al., 1981), — — — observed (Hoyt, 1976), ····· Exp. 15I, ——— Exp. 22.

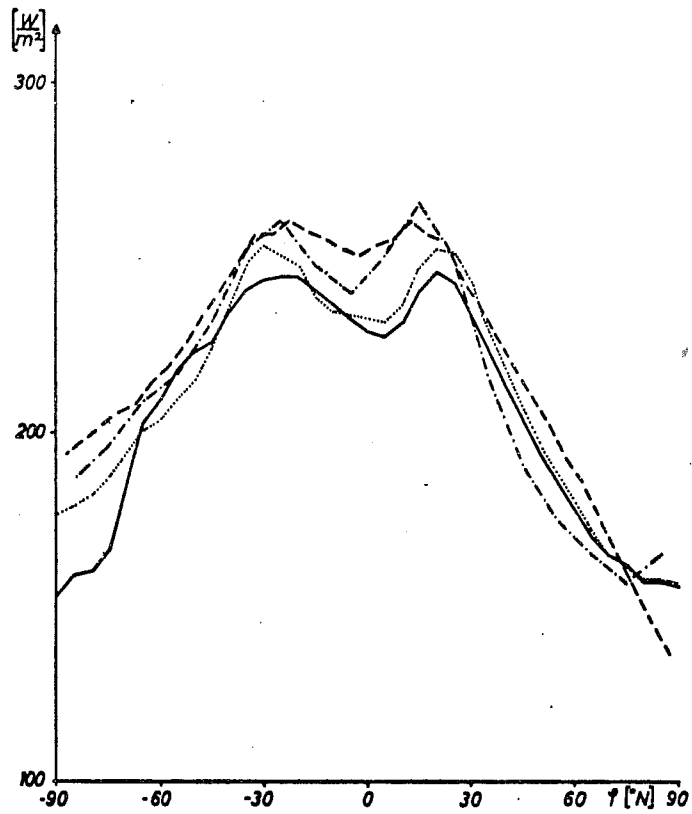

Figure 10: January zonal mean outgoing longwave radiation, notation as in Fig. 9.

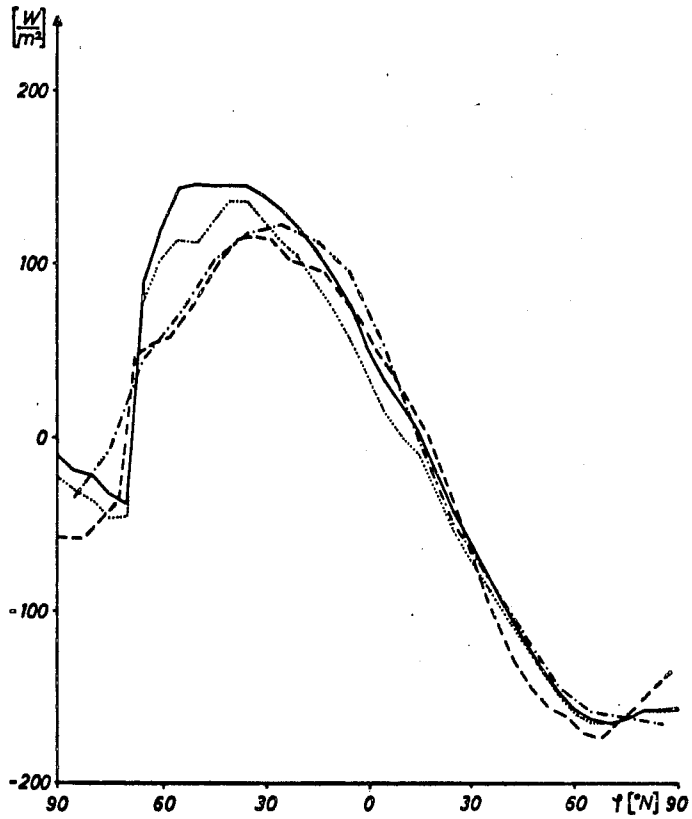

Figure 11: January zonal mean radiation balance at the top of the atmosphere, notation as in Fig. 9.

6. OUTLOOK

At the present stage of development the Sasamori-scheme in some points seems to be slightly superior to the ECMWF-scheme. Additionally, it offers some possibilities for further development:

- Using vertical profiles for the time constants τ_w and τ_p might improve the results.
- The results might also be improved by using a parameterization of the standard deviation of vertical velocity, which is based on physical considerations.
- In principle the necessary incorporation of convective cloud cover and liquid water content may be handled by the same scheme. This requires the determination of mean vertical velocities and - particularly - standard deviations of vertical velocity characteristic of convection.
- Since not only cloud cover and liquid water content but also condensation rate and precipitation rate are supplied by the scheme, the whole hydrologic cycle of the atmosphere could be parameterized by only one scheme. But of course it remains uncertain whether this - surely attractive - joining of cloud cover and hydrologic cycle computations will yield realistic results.

7. References

Berlyand,T.G. and L.A.Strokina, 1980: Global distribution of a cumulative number of clouds. Leningrad, Gidrometeoizdat

Burridge,D.M. and J.Haseler, 1977: A model for medium range weather forecasting - Adiabatic formulation. ECMWF Technical Report No. 4, 46 pp.

Geleyn,J.F., 1981: Some diagnostics of the cloud/radiation interaction in ECMWF forecasting model. In: 'ECMWF Workshop on Radiation and Cloud-Radiation Interaction in Numerical Modelling', 135

Hense,A., 1982: Wolkenparametrisierungen in Zirkulationsmodellen. Mitt. Inst. Geophys. und Meteor. der Univ. zu Köln, Nr. 35, 91 pp

Hense,A. and E.Heise, 1984: A sensitivity study of cloud parameterizations in general circulation models. Beitr. Phys. Atm., 57, 240 - 258 Paper I

Hense,A.,M.Kerschgens and E.Raschke, 1982: An economical method for computing the radiative energy transfer in circulation models. Quart. Journ. Roy. Met. Soc., 108, 231 - 252

Hoyt,D.V., 1976: The radiation and energy budgets of the earth using both ground-based and satellite-derived values of total cloud cover. NOAA Techn. Report ERL 362-ARL 4, 124 pp

Jacobsen,I. and E.Heise, 1982: A new economic method for the computation of the surface temperature in numerical models. Beitr. Phys. Atm., 55, 128 - 141

Njoku,E.G. and L.Swanson, 1983: Global measurements of sea surface temperature, wind speed and atmospheric water content from satellite microwave radiometry. Mon. Weath. Rev., 111, 1977 - 1987

Sasamori,T., 1975: A statistical model for stationary atmospheric cloudiness, liquid water content, and rate of precipitation. Mon. Weath. Rev., 103, 1037 - 1049

Smagorinsky,J., 1960: On the numerical prediction of large scale condensation by numerical models. Geophys. Monogr. No. 5, Amer. Geophys. Union, Washington, D.C., 71 - 78

Stephens,G.L.,G.G.Campbell and T.H.Vonder Haar, 1981: Earth radiation budgets. Journ. Geophys. Res., 86, C10, 9739 - 9760

Tiedtke,M. and J.F.Geleyn, 1975: The DWD general circulation model - Description of its main features. Beitr. Phys. Atm., 48, 255 - 277